^{18}F-FDG PET Early Response Evaluation of Locally Advanced Non–Small Cell Lung Cancer Treated with Concomitant Chemoradiotherapy

Edwin A. Usmanij[1,2], Lioe-Fee de Geus-Oei[1], Esther G.C. Troost[2], Liesbeth Peters-Bax[3], Erik H.F.M. van der Heijden[4], Johannes H.A.M. Kaanders[2], Wim J.G. Oyen[1], Olga C.J. Schuurbiers[4], and Johan Bussink[2]

[1]Department of Nuclear Medicine, Radboud University Nijmegen Medical Centre, Nijmegen, The Netherlands; [2]Department of Radiation Oncology, Radboud University Nijmegen Medical Centre, Nijmegen, The Netherlands; [3]Department of Radiology, Radboud University Medical Centre, Nijmegen, The Netherlands; and [4]Department of Pulmonary Diseases, Radboud University Nijmegen Medical Centre, Nijmegen, The Netherlands

The potential of ^{18}F-FDG PET changes was evaluated for prediction of response to concomitant chemoradiotherapy in patients with locally advanced non–small cell lung cancer (NSCLC). **Methods:** For 28 patients, ^{18}F-FDG PET was performed before treatment, at the end of the second week of treatment, and at 2 wk and 3 mo after the completion of treatment. Standardized uptake value (SUV), maximum SUV, metabolic tumor volume (MTV), and total lesion glycolysis (TLG) were obtained. Early metabolic changes were defined as fractional change (ΔTLG) when ^{18}F-FDG PET at the end of the second week was compared with pretreatment ^{18}F-FDG PET. In-treatment metabolic changes, as measured by serial ^{18}F-FDG PET, were correlated with standard criteria of response evaluation of solid tumors by means of CT imaging (Response Evaluation Criteria In Solid Tumors 1.1). Parameters were analyzed for stratification in progression-free survival (PFS). **Results:** When compared with early metabolic nonresponders, a ΔTLG decrease of 38% or more was associated with a significantly longer PFS (1-y PFS 80% vs. 36%, $P = 0.02$). Pretreatment TLG was found to be a prognostic factor for PFS. **Conclusion:** The degree of change in TLG was predictive for response to concomitant chemoradiotherapy as early as the end of the second week into treatment for patients with locally advanced NSCLC. Pretreatment TLG was prognostic for PFS.

Key Words: early response prediction; non–small cell lung cancer; concomitant radiotherapy chemotherapy; ^{18}F-FDG PET; standardized uptake value; total lesion glycolysis

Management of patients with locally advanced non–small cell lung cancer (NSCLC) has changed significantly in the past few years (*1,2*). Concomitant chemoradiotherapy is the standard of care in fit patients (Eastern Cooperative Oncology Group [ECOG] performance status grade, 0–1) (*3*). However, intensification of

treatment significantly increases morbidity while yielding modest improvements in terms of overall survival (*3*). If a good response is obtained after chemoradiotherapy, surgery with curative intent can be beneficial (*4*) but only if a complete eradication of vital tumor cells in involved lymph nodes is achieved. On the other end, there are some patients who do not respond to chemoradiotherapy yet they still experience the side effects (*3*). With recent developments in dose escalation in NSCLC, a further increase in toxicity is reported (*5,6*). Therefore, a need arises to predict therapy response at an early phase on an individual-patient basis, possibly leading to improved tumor control, a reduction in side effects, and eventually avoidance of futile costs of ineffective treatment (*7*).

Imaging of treatment response is mainly static, based on the assessment of tumor size on CT and classification of metric changes using international Response Evaluation Criteria In Solid Tumors (RECIST) (*8*). However, these morphologic methods are of limited value for detection of an early therapy response. Anatomic imaging cannot distinguish atelectasis or fibrotic tissue from residual tumor (*9,10*). Consequently, radiographic response does not show correlation with histopathologic regression after neoadjuvant chemoradiotherapy in NSCLC (*11*). Thus, response assessment by standard radiologic imaging is only meaningful after the end of therapy, when the opportunity to modify possible ineffective treatment has passed. Functional imaging using ^{18}F-FDG PET has gained widespread acceptance for diagnosis and staging in oncology and has proven prognostic value for NSCLC (*12*). The application of ^{18}F-FDG PET for the prediction of therapy response and treatment outcome has been shown in advanced stage NSCLC during induction chemotherapy (*13–16*), during radiotherapy (*17*), and after neoadjuvant chemotherapy (*18*). Data for response prediction of ^{18}F-FDG PET in locally advanced NSCLC treated with concomitant therapy are limited. The aim of this study was to assess the predictive value of ^{18}F-FDG PET in locally advanced NSCLC, performed after 2 wk of concomitant chemoradiotherapy. We hypothesized that early treatment–induced glucose metabolic changes, measured by ^{18}F-FDG PET scans, can predict clinical outcome.

MATERIALS AND METHODS

Patients

From January 2008 to January 2012, patients with newly diagnosed locally advanced NSCLC eligible for concomitant chemoradiotherapy were enrolled in this study. Inclusion criteria were cytologically or

histologically proven NSCLC stage IIIA (TNM sixth edition, Union for International Cancer Control [UICC], T3 or N2) or stage IIIB (TNM sixth edition, UICC, T4 or N3); age, 18–80 y; and ECOG performance status grade, 0–1. The exclusion criterion was previous thoracic radiotherapy. The study was approved by the Institutional Review Board of the Radboud University Nijmegen Medical Centre. All patients gave written informed consent.

Treatment

Patients were treated with chemoradiotherapy in a concomitant scheme. An intensity-modulated radiotherapy technique was delivered to a total dose of 66 Gy in 33 fractions of 2 Gy, 5 fractions per week, using 10-MV photons. The gross tumor volume consisted of the primary tumor and involved hilar or mediastinal lymph nodes (i.e., PET-positive or cytologically proven lymph nodes). The clinical target volume contained gross tumor volume plus a 1.0-cm margin for the primary tumor and 0.5-cm margin for the lymph nodes. The planning target volume consisted of the clinical target volume plus a 0.5-cm margin. The chemotherapy regimen consisted of 2 cycles of cisplatin (50 mg/m^2 of body surface area [days 1 and 8 of the first cycle and days 22 and 29 of the second cycle]) and etoposide (100 mg/m^2 of body surface area intravenously [days 1–3 of the first cycle and days 22–24 of the second cycle]), starting on the first day of radiotherapy. The planned overall treatment period was 45 d.

Staging and Follow-up

All patients underwent diagnostic work-up, including contrast-enhanced CT of the thorax and upper abdomen; whole-body ^{18}F-FDG PET/CT; MR imaging of the brain; bronchoscopy with transbronchial needle aspiration (TBNA), esophageal ultrasound fine-needle aspiration (EUS-FNA), or endobronchial ultrasound with TBNA (EBUS-TBNA); and mediastinoscopy in the case of PET-positive, cytologically negative mediastinal lymph nodes. After work-up, all patients were discussed in a thoracic oncology multidisciplinary board. Before chemoradiotherapy, ^{18}F-FDG PET/CT of the thorax was performed in radiotherapy position for radiotherapy planning (median interval, 11 d; range, 1–27 d).

Early response measurement, using ^{18}F-FDG PET/CT, was performed at the beginning of week 3 (after a median dose of 20 Gy; range, 20–24 Gy), always before the second chemotherapy cycle. All attending physicians were masked to the results of this early response ^{18}F-FDG PET/CT examination, which was part of the study protocol. Therefore, study data did not affect treatment decisions. The study design is shown in Figure 1.

[Fig. 1]

Two to 3 wk after the end of therapy (median, 19 d; range, 14–21 d), patients were restaged with whole-body ^{18}F-FDG PET/CT and contrast-enhanced CT of the chest and upper abdomen. All tumor response was assessed according to RECIST 1.1 (8). If findings indicated an objective response to therapy and the primary tumor was considered resectable by lobectomy and if patients were considered operable, restaging of mediastinal nodes by EUS or EBUS was performed, followed by mediastinoscopy in the case of negative cytology (normal cytologic lymph node punctate or nonrepresentative punctures). Patients underwent lobectomy in the case of complete mediastinal histopathologic response (i.e., cytologically or histologically no vital tumor cells in previously affected nodes). In the case of persistent N2 disease or if patients were not eligible for surgery (tumor unresectablity or inoperable patients), follow-up was performed.

Final treatment response after chemoradiotherapy was assessed using ^{18}F-FDG PET 3 mo after treatment (range, 2–5 mo) in the nonsurgical group. Follow-up during and after treatment for all patients consisted of standard follow-up according to the following international guidelines: clinical examination at regular intervals (every 3 mo in the first year), chest-x-rays, and chest CT scans if clinically indicated.

^{18}F-FDG PET/CT Scan

All PET investigations were performed with a hybrid PET/CT scanner (Biograph Duo Siemens Medical Solutions USA, Inc.) according to guidelines of the European Association of Nuclear Medicine (19). Patients fasted for at least 6 h. Blood glucose levels were lower than 8.2 mmol/L in all patients (mean, 6.0 mmol/L). According to protocol, 60 min (mean ± SD, 77.94 ± 9.1 min) after intravenous injection of ^{18}F-FDG (3.45 MBq/kg; Covidien) and furosemide (10 mg), static emission scans in 3-dimensional mode were obtained, covering the neck, thorax, abdomen, and pelvis. The PET acquisition time was 4 min per bed position. The second and third ^{18}F-FDG PET scans were obtained covering the thorax only. PET scans were processed using iterative reconstruction with the ordered-subsets expectation maximization algorithm (image matrix size, 128 × 128; 4 iterations, 16 subsets; and a 5-mm 3-dimensional gaussian filter). The reconstructed images were corrected for injected dose, decay of ^{18}F-FDG, patient body weight, and attenuation using a low-dose CT-scan.

Standardized Uptake Value (SUV) and Total Lesion Glycolysis (TLG)

PET and CT scans were imported into Pinnacle^3 (version 8.0 d; Philips Radiation Oncology Systems). All SUVs were derived from the ^{18}F-FDG PET scans using semiautomatic delineation techniques. ^{18}F-FDG uptake was calculated as maximum SUV (SUV_{max}) within the metabolic active tumor volume (MTV) of the primary tumor and mean SUV. MTVs were delineated using 50% isocontour thresholds based on a fixed percentage of the maximum activity within the lesion, without background correction. Metastatic lymph nodes were analyzed separately using a 50% method. Volume-weighted mean values of SUV in all ^{18}F-FDG–avid lesions per PET scan were derived to provide 1 value for each study. TLG was calculated using a summation of SUV × MTV (cm^3), including both the primary tumor and all metastatic lymph nodes.
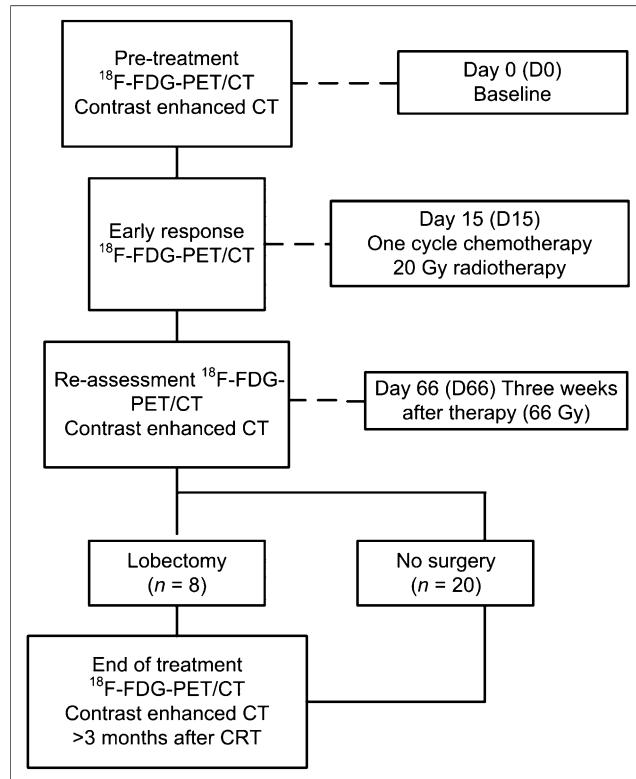

FIGURE 1. Study design. CRT = chemoradiotherapy.

jnm116921-pm ■ 7/17/13

TABLE 1
Patient Characteristics

Characteristic	Value
Age (y)	
Mean	59
Range	41−77
Age < 65	15 (54%)
Age ≥ 65	13 (46%)
Sex	
Male	18 (64%)
Female	10 (36%)
Histology	
Squamous cell carcinoma	11 (39%)
Adenocarcinoma	14 (50%)
Non–small cell (not other specified)	3 (11%)
TNM stage (sixth edition)	
IIIA	17 (61%)
T0N2	1 (4%)
T1N2	3 (11%)
T2N2	8 (29%)
T3N2	5 (18%)
IIIB	11 (39%)
T1N3	3 (11%)
T2N3	1 (4%)
T4N0	3 (11%)
T4N2	2 (7%)
T4N3	2 (7%)
Performance score (ECOG)	
0	20 (71%)
1	8 (29%)
Smoking status	
Current smoker	12 (43%)
Former smoker	16 (57%)
Previous malignancy	
No	24 (86%)
Yes	4 (14%)
Adjuvant surgery	
No surgery	20 (71%)
Lobectomy	8 (29%)

RESULTS

Patients Characteristics and Follow-up

Thirty patients were included. Two patients were excluded, because they did not receive an appropriate early in-treatment ^{18}F-FDG PET scan. Patient characteristics are summarized in Table 1. [Table 1] All patients received 60–66 Gy of radiotherapy and 2 cycles of chemotherapy. Total median treatment time was 45 d (range, 43–49 d). The end-of-treatment reassessment according to RECIST 1.1 revealed 16 patients as responders (complete responders, 0; partial responders, 16) and 12 patients as nonresponders (stable disease, 11; progressive disease, 1). Seven patients, successfully pathologically downstaged and considered resectable, received a lobectomy. Protocol violation took place in 1 patient with persistent N2 disease (1 level). Thus, a total of 8 patients underwent lobectomy, with complete tumor resection (R0) in 7 of 8 patients. Pathologic assessment showed ypT0N0M0 status in 4 of 8 patients. Four patients showed residual viable tumor cells in the resected lobe, including the patient with persistent N2 disease.

Clinical Follow-up

The patient outcome data for time to progression was defined as the interval between the start of treatment and the date of documented disease progression as confirmed by imaging or biopsy. If a patient was progression-free at the closeout date (May 29, 2012), time to progression was censored to that date. Overall survival was measured from the date of treatment start to death. Patients still alive at the closeout date were censored for survival at that date.

Data and Statistical Analysis

All CT images were read by 1 experienced radiologist, who was masked for the early response PET data. The PET scans were read by consensus of 2 experienced nuclear medicine physicians. Regions of interest were defined using semiautomatic scripts, after input of target region of interest. The radiologists and nuclear physicians were masked to clinical outcome. Variation in parameters in sequential scans was normalized to baseline: $\Delta = $ (pretreatment – in treatment)/ pretreatment $\times 100\%$.

Univariate analysis for progression-free survival (PFS) was performed on TLG, SUV, and TNM parameters. All SUV and TLG parameters were analyzed as continuous variables. Variable selection for multivariate analysis was performed by both forward and backward stepwise covariate selection. The hazard ratio (HR) per unit parameter change and its 95% confidence interval were reported, unless indicated

TABLE 2
TLG Evolution Sorted by TNM Subgroups

TNM stage (sixth edition)	n	Pretreatment TLG	In-treatment TLG	ΔTLG (%)
IIIA (n = 17)				
T0N2	1 (4)	83.60	26.93	−67.79
T1N2	3 (11)	27.35	15.34	+ 43.91
		127.97	108.18	−15.46
		6.33	3.27	−48.31
T2N2	8 (29)	156.81	59.93	−61.78
		323.93	278.08	−14.16
		199.1	48.63	−75.57
		31.83	30.05	−5.59
		60.21	76.13	+26.45
		92.89	51.88	−44.15
		72.18	45.47	−37.00
		243.41	92.01	−62.20
T3N2	5 (18)	188.80	145.7	−22.83
		339.14	68.61	−79.77
		95.80	64.47	−32.70
		233.48	108.07	−53.71
		717.87	624.52	−13.00
IIIB (n = 11)				
T1N3	3 (11)	263.68	398.50	+51.13
		49.79	20.44	−58.94
		163.20	74.16	−54.56
T2N3	1 (4)	224.42	84.67	−62.27
T4N0	3 (11)	77.19	36.98	−52.10
		199.84	26.00	−86.99
		676.20	416.06	−38.47
T4N2	2 (7)	489.18	174.15	−64.40
		1319.04	1042.25	−20.98
T4N3	2 (7)	339.64	177.56	−47.72
		210.71	152.9	−27.43

Data in parentheses are percentages.

TABLE 3
Univariate Analysis Covariates and Effect on PFS (per Unit Change)

PET parameter	HR	95% confidence interval	P
Pretreatment TLG	1.005	1.002–1.007	0.004
In-treatment TLG	1.005	1.003–1.008	0.001
ΔTLG	1.016	1.002–1.030	0.025
Pretreatment SUV	Not significant	0.999–1.002	0.575
In-treatment SUV	Not significant	0.999–1.003	0.327
ΔSUV	Not significant	0.995–1.022	0.231
Pretreatment SUV_{max}	Not significant	0.999–1.000	0.447
In-treatment SUV_{max}	Not significant	0.999–1.002	0.579
ΔSUV_{max}	Not significant	0.998–1.027	0.087
TNM (IIIA–IIIB)	Not significant	0.299–2.136	0.655

Median follow-up was 16 mo (range, 4–34 mo), for the surviving patients 17 mo (range, 4–34 mo) and for deceased patients 10 mo (range, 4–23 mo). During follow-up, 9 patients died, all related to cancer progression. Overall survival at 1 and 2 y was 76% and 28%, respectively. Sixteen patients developed recurrent disease, 3 with progression of local disease, whereas distant metastases were detected in 13 patients (cerebral, $n = 9$; liver, $n = 1$; adrenal gland, $n = 1$; skin, $n = 1$; and bone, $n = 1$). Median time to progression was 12 mo. PFS after treatment start was 62% after 1 y and 19% after 2 y.

TLG and PFS

Pretreatment TLG was 250.48 (±274.54) for the whole study group, whereas in-treatment TLG was 158.96 (±224.33). In stage IIIA patients, mean pretreatment and in-treatment TLG were 176.51 (±171.59) and 108.66 (±147.26), respectively, whereas stage IIIB patients had a mean TLG of 364.81 (±364.30) and 236.70 (±300.38). An overview of baseline TLG, in-treatment TLG, and ΔTLG for all patients is shown in Table 2. Univariate Cox regression analysis for PFS was used to analyze the relationships between covariates of interest (Table 3). Significant parameters for PFS were pretreatment TLG, in-treatment TLG, and ΔTLG. When ΔTLG for pretreatment TLG was corrected, both factors remained significant for PFS (Table 4). A 10% less decrease in ΔTLG was associated with an HR of 1.169 ($P = 0.033$) for PFS. Every 10-unit increase from baseline TLG index was associated with an HR of 1.047 ($P = 0.009$).

To avoid data-driven significance for cutoff, ΔTLG was stratified at the median level. At a median level of 45% cutoff, patients with less than 45% decrease in ΔTLG ($n = 14$) had a median PFS of 9.8 mo, whereas patients with a 45% or more decrease in ΔTLG ($n = 14$) had a median PFS of 15.9 mo ($P = 0.032$, log-rank test). PFS beyond 2 y occurred only in patients with a 38% or more decrease in ΔTLG. The Kaplan–Meier curve for PFS at a median cutoff ΔTLG is shown in Figure 2, and PFS data at various cutoff points is shown in Table 5.

PFS was eventually stratified by the following 3 risk groups: favorable (baseline TLG < 500 and ≥38% decrease in ΔTLG),

intermediate (baseline TLG < 450 or ≥38% decrease in ΔTLG), and unfavorable (baseline TLG ≥ 450 and <38% decrease in ΔTLG). A Kaplan–Meier curve of stratified risk groups is shown in Figure 3. Median survival in the favorable group was 17 mo (range, 45.9–34.0 mo), whereas in the intermediate group median survival was 11.8 mo (range, 3.3–31.7 mo). The unfavorable group had a median survival of 2.3 mo (range, 2.1–4.5 mo).

Figure 4 shows an example of 2 patients with sequential scans. Because ΔSUV showed similar decrease, the difference in ΔTLG was apparent.

DISCUSSION

In the present prospective study, we investigated the predictive value of metabolic change assessed by ^{18}F-FDG PET in locally advanced NSCLC treated with concomitant chemoradiotherapy. Pretreatment and early in-treatment ^{18}F-FDG PET scans were compared with clinical outcome. Proportional hazards analysis revealed that a smaller decrease in ΔTLG was associated with earlier disease progression. Despite our relatively small study group of 28 patients, ΔTLG showed significant association with PFS. For a broad range of cutoff points in ΔTLG, with a corresponding range of 38%–52% decrease in ΔTLG, a significantly different log-rank probability between strata for PFS was repeatedly found ($P < 0.05$). However, early metabolic response did not show significant association with overall survival ($P = 0.10$). The absence

TABLE 4
Analysis of PFS, with ΔTLG Corrected for Pretreatment TLG (per 10 Unit Change)

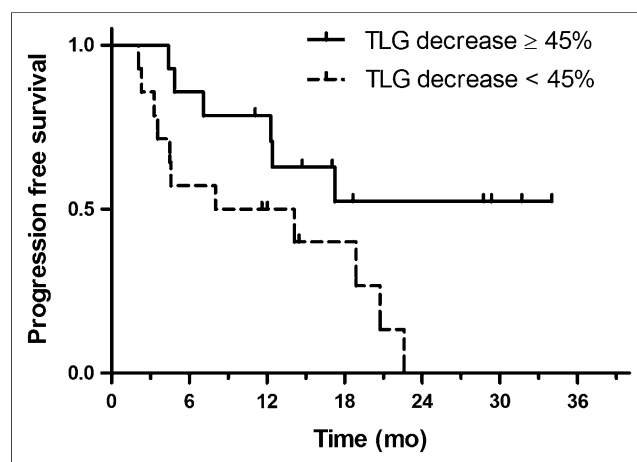| PET parameter	HR	95% confidence interval	P
ΔTLG	1.169	1.013–1.350	0.033
Pretreatment TLG	1.047	1.020–1.076	0.009

FIGURE 2. Kaplan–Meier analysis of PFS at median cutoff in ΔTLG. Median, 1-y, and 2-y PFS was 15.9 mo, 73%, and 40%, respectively, for ΔTLG decrease ≥ 45% vs. 9.8 mo, 46%, and 0%, respectively, for ΔTLG decrease < 45% (log-rank test, $P = 0.032$).

TABLE 5
PFS at Various Cutoff Points in ΔTLG

PFS	Median PFS (mo)	1-y PFS (%)	2-y PFS (%)	P
All patients	15.7	76	28	
ΔTLG decrease < 38% (n = 12)	6.3	36	0	0.020
ΔTLG decrease ≥ 38% (n = 16)	15.9	80	33	
ΔTLG decrease < 45% (n = 14)	9.8	46	0	0.032
ΔTLG decrease ≥ 45% (n = 14)	15.9	73	40	
ΔTLG decrease < 52% (n = 16)	9.8	47	0	0.035
ΔTLG decrease ≥ 52% (n = 12)	17.1	82	44	

of a significant correlation can at least partly be explained by the relatively short follow-up in this study.

Another finding was that pretreatment TLG was prognostic for PFS. Only recently has the prognostic value of TLG in NSCLC been elucidated (20–22). Chen et al. (20) demonstrated that a whole-body TLG is a potentially useful indicator for PFS in NSCLC, because a high whole-body TLG (>655) is associated with poor prognosis. Concerning our study, one might reasonably question whether pretreatment TLG was correlated with ΔTLG, arguing that a high-baseline TLG tends to show more decrease during treatment than lesions with low TLG. However, expression as a fractional change overcomes this issue by expressing ΔTLG as fractional change from baseline. Furthermore, we showed in Cox regression that both ΔTLG and pretreatment TLG remained significant for PFS. This significance indicates that both factors are independently associated with PFS, pretreatment TLG being prognostic for survival before treatment, whereas ΔTLG is predictive of treatment response.

We can only hypothesize about the different trends in ΔTLG between patients. As treatment starts, the time course in ^{18}F-FDG uptake is dependent on many factors. First, a decrease in ^{18}F-FDG tumor uptake is expected from both tumor cell kill and a reversible metabolic effect (caused by quiescence of tumor cells) while the cells remain viable (23). Second, an increase in metabolic activity is expected from increased tumor cell repopulation, inflammation, and tumor-resistance mechanisms. Because radiation requires oxygen for its cytotoxic effects, cellular metabolism is changed under hypoxic conditions. Via upregulation of hypoxia-inducible factor 1α, change in cellular metabolism under hypoxic conditions

leads to increased glycolysis, with subsequent increased demand of glucose leading to upregulation of glucose transporters and eventually increased ^{18}F-FDG uptake (24–26). Because a high hypoxia-inducible factor 1α expression in NSCLC is associated with an earlier disease progression (27), we suspect resistance mechanisms to be correlated with less decrease in ΔTLG.

Unreliable outcome prediction of the end-of-treatment ^{18}F-FDG PET scans was most likely caused by postradiotherapy changes (28): ^{18}F-FDG uptake is not limited to accumulation in tumor tissue, but it also accumulates in macrophages, neutrophils, fibroblast, and granulation tissue (29). Multiple biologic processes such
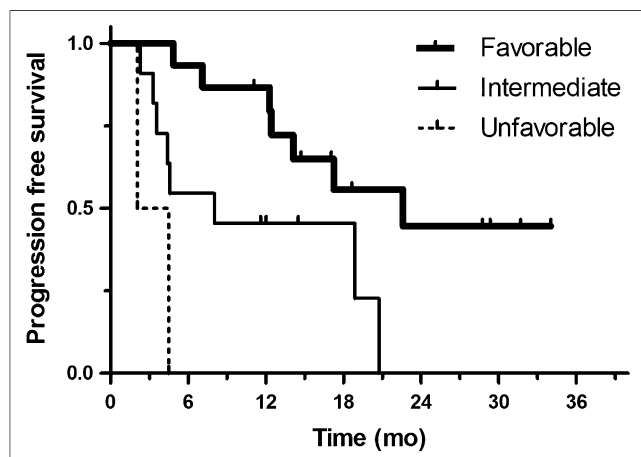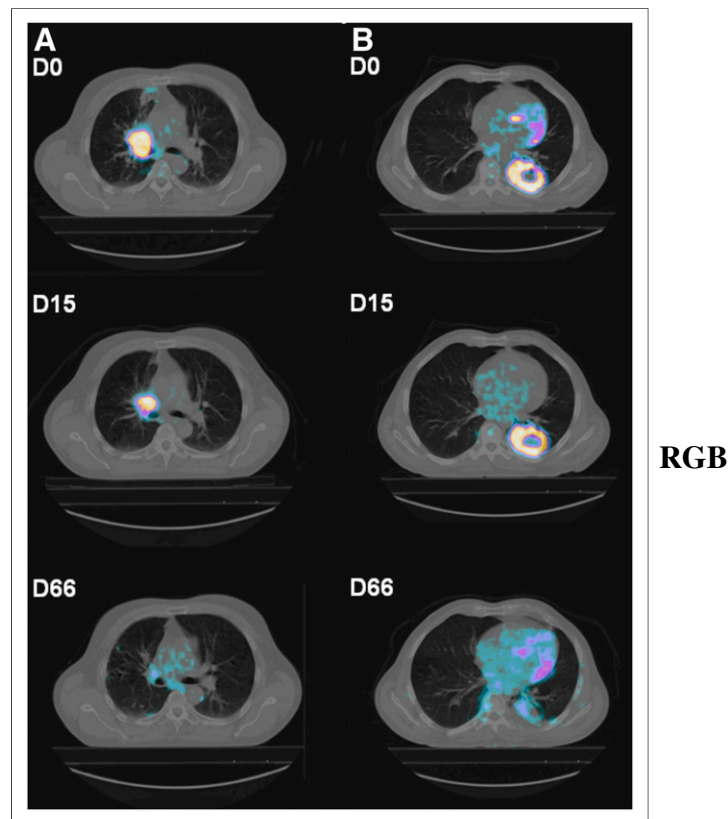
RGB

FIGURE 4. Typical example of 2 patients with stage III NSCLC and their sequential ^{18}F-FDG PET/CT scans: pretreatment (D0), intreatment (D15), and end of treatment (D66). Two weeks into concomitant chemoradiotherapy, patient A showed 14% decrease in in-treatment SUV, and 54% decrease in TLG, censored for both overall survival and PFS at 19 mo. Patient B showed 14% decrease in in-treatment SUV and TLG, PFS of 12 mo, and overall survival of 16 mo. All series are shown using equal window scaling.

FIGURE 3. Kaplan–Meier analysis of favorable, intermediate, and unfavorable risk groups (log-rank test, P < 0.02).

as proliferation, cell repair, and inflammation may conceal vital tumor residue. Serial follow-up PET/CT 3 and 6 mo after treatment was performed to evaluate the evolution of ^{18}F-FDG uptake and postirradiation inflammation. Using an in-treatment scan as early as 2-wk therapy possibly avoids confounding effects of multiple biologic processes. We suggest that at the second week, a metabolic tumor effect is at play, whereas other non–tumor-related biologic processes have a less significant role in the second week. A significant decrease in ^{18}F-FDG uptake and volume might suggest tumor response to therapy.

Studies addressing response prediction using early in-treatment ^{18}F-FDG PET in locally advanced (stage III) NSCLC treated with concomitant therapy are limited. A previous study by Huang et al. (30) in stage III and IV NSCLC found that ^{18}F-FDG PET after 3 wk (and 40 Gy) of concomitant chemoradiotherapy therapy had preceded morphologic response. However, no effect on PFS and overall survival was presented. Macchessi et al. (31) showed in unresectable stage II and III NSCLC no correlation for metabolic change on in-treatment ^{18}F-FDG PET and clinical outcome. The relatively wide range (10–25 d relative to 10–12 d in our study) of the second scan may have hampered the study. By applying TLG, both volumetric (MTV) and metabolic information (SUV) are incorporated, resulting in a more sensitive method for detection of treatment response relative to SUV alone. The general concept of using TLG and ΔTLG for tumor treatment response was first introduced by Larson et al. (32), who calculated ΔTLG as a response index, also called the Larson–Ginsberg index. To our knowledge, the present study is the first study to show the predictive value of ΔTLG for early response monitoring in locally advanced NSCLC treated with concomitant chemoradiotherapy. Despite the promising results, the small number of patients and a large heterogeneity in metabolic tumor activity are limiting factors. We could not investigate the reliability of response monitoring in small tumors (i.e., <1 cm) or tumors with low metabolic uptake, in which a variety of technical factors may hamper adequate and reproducible calculation of the fractional change in tumor lesion glycolysis. However, by implementing standard methods of data analysis, the use of ^{18}F-FDG PET early during treatment seems clinically feasible. One major restriction of the current study was the relatively small amount of patients included. Even though TLG displayed prognostic and predictive potential in univariate analysis, a robust multivariate analysis, correcting for known prognostic factors (i.e., age, histology, disease stage, performance status), remained unexplained. Therefore, other confounding factors cannot be fully excluded by this study.

Consequently, confirmation of our findings is needed in larger study populations. Also, research is needed to further individualize treatment in stage III non–small cell lung cancer. Patients showing early metabolic nonresponse could prove to be candidates for dose escalation regimes, possibly improving clinical outcome (33). These kinds of studies set the basis for PET-based response–adapted treatment algorithms, which are the promise of the near future; the choice of therapy, its intensity, and its duration will become better adjusted to the biology of the individual patient.

CONCLUSION

The current study in locally advanced NSCLC patients treated with concomitant chemoradiotherapy indicates that early in-treatment ^{18}F-FDG PET can be used to predict outcome. The effect of combined treatment does not preclude its predictive capabilities, because we found ΔTLG was predictive of PFS. Both pretreatment TLG and the degree of change in TLG may be useful tools for individualizing treatment in locally advanced NSCLC.

DISCLOSURE

REFERENCES

1. El-Sharouni SY, Kal HB, Battermann JJ, Schramel FM. Sequential versus concurrent chemo-radiotherapy in inoperable stage III non-small cell lung cancer. *Anticancer Res.* 2006;26:495–505.
2. Govindan R, Bogart J, Vokes EE. Locally advanced non-small cell lung cancer: the past, present, and future. *J Thorac Oncol.* 2008;3:917–928.
3. Aupérin A, Le Pechoux C, Rolland E, et al. Meta-analysis of concomitant versus sequential radiochemotherapy in locally advanced non-small-cell lung cancer. *J Clin Oncol.* 2010;28:2181–2190.
4. Albain KS, Swann RS, Rusch VW, et al. Radiotherapy plus chemotherapy with or without surgical resection for stage III non-small-cell lung cancer: a phase III randomised controlled trial. *Lancet.* 2009;374:379–386.
5. van Baardwijk A, Reymen B, Wanders S, et al. Mature results of a phase II trial on individualised accelerated radiotherapy based on normal tissue constraints in concurrent chemo-radiation for stage III non-small cell lung cancer. *Eur J Cancer.* 2012;48:2339–2346.
6. Machtay M, Bae K, Movsas B, et al. Higher biologically effective dose of radiotherapy is associated with improved outcomes for locally advanced non-small cell lung carcinoma treated with chemoradiation: an analysis of the Radiation Therapy Oncology Group. *Int J Radiat Oncol Biol Phys.* 2012;82:425–434.
7. Bussink J, Kaanders JH, van der Graaf WT, Oyen WJ. PET-CT for radiotherapy treatment planning and response monitoring in solid tumors. *Nat Rev Clin Oncol.* 2011;8:233–242.
8. Eisenhauer EA, Therasse P, Bogaerts J, et al. New response evaluation criteria in solid tumours: revised RECIST guideline (version 1.1). *Eur J Cancer.* 2009;45:228–247.
9. Wahl RL, Jacene H, Kasamon Y, Lodge MA. From RECIST to PERCIST: evolving considerations for PET response criteria in solid tumors. *J Nucl Med.* 2009; 50:122S–150S.
10. Mac Manus MP, Hicks RJ, Matthews JP, et al. Positron emission tomography is superior to computed tomography scanning for response-assessment after radical radiotherapy or chemoradiotherapy in patients with non-small-cell lung cancer. *J Clin Oncol.* 2003;21:1285–1292.
11. Liu-Jarin X, Stoopler MB, Raftopoulos H, Ginsburg M, Gorenstein L, Borczuk AC. Histologic assessment of non-small cell lung carcinoma after neoadjuvant therapy. *Mod Pathol.* 2003;16:1102–1108.
12. de Geus-Oei LF, van der Heijden HF, Corstens FH, Oyen WJ. Predictive and prognostic value of FDG-PET in nonsmall-cell lung cancer: a systematic review. *Cancer.* 2007;110:1654–1664.
13. Lee DH, Kim SK, Lee HY, et al. Early prediction of response to first-line therapy using integrated ^{18}F-FDG PET/CT for patients with advanced/metastatic non-small cell lung cancer. *J Thorac Oncol.* 2009;4:816–821.
14. Vansteenkiste JF, Stroobants SG, De Leyn PR, Dupont PJ, Verbeken EK. Potential use of FDG-PET scan after induction chemotherapy in surgically staged IIIa-N2 non-small-cell lung cancer: a prospective pilot study. The Leuven Lung Cancer Group. *Ann Oncol.* 1998;9:1193–1198.
15. Nahmias C, Hanna WT, Wahl LM, Long MJ, Hubner KF, Townsend DW. Time course of early response to chemotherapy in non-small cell lung cancer patients with ^{18}F-FDG PET/CT. *J Nucl Med.* 2007;48:744–751.
16. Weber WA, Petersen V, Schmidt B, et al. Positron emission tomography in non-small-cell lung cancer: prediction of response to chemotherapy by quantitative assessment of glucose use. *J Clin Oncol.* 2003;21:2651–2657.
17. van Baardwijk A, Bosmans G, Dekker A, et al. Time trends in the maximal uptake of FDG on PET scan during thoracic radiotherapy: a prospective study in locally advanced non-small cell lung cancer (NSCLC) patients. *Radiother Oncol.* 2007;82:145–152.
18. de Geus-Oei LF, van der Heijden HF, Visser EP, et al. Chemotherapy response evaluation with ^{18}F-FDG PET in patients with non-small cell lung cancer. *J Nucl Med.* 2007;48:1592–1598.

19. Boellaard R, O'Doherty MJ, Weber WA, et al. FDG PET and PET/CT: EANM procedure guidelines for tumour PET imaging—version 1.0. *Eur J Nucl Med Mol Imaging.* 2010;37:181–200.

20. Chen HH, Chiu NT, Su WC, Guo HR, Lee BF. Prognostic value of whole-body total lesion glycolysis at pretreatment FDG PET/CT in non-small cell lung Cancer. *Radiology.* 2012;264:559–566.

21. Zhang H, Wroblewski K, Liao S, et al. Prognostic value of metabolic tumor burden from ^{18}F-FDG PET in surgical patients with non-small-cell lung cancer. *Acad Radiol.* 2013;20:32–40.

22. Liao S, Penney BC, Wroblewski K, et al. Prognostic value of metabolic tumor burden on ^{18}F-FDG PET in nonsurgical patients with non-small cell lung cancer. *Eur J Nucl Med Mol Imaging.* 2012;39:27–38.

23. Patz EF Jr, Connolly J, Herndon J. Prognostic value of thoracic FDG PET imaging after treatment for non-small cell lung cancer. *AJR.* 2000;174:769–774.

24. Moeller BJ, Cao Y, Li CY, Dewhirst MW. Radiation activates HIF-1 to regulate vascular radiosensitivity in tumors: role of reoxygenation, free radicals, and stress granules. *Cancer Cell.* 2004;5:429–441.

25. Meijer TW, Kaanders JH, Span PN, Bussink J. Targeting hypoxia, HIF-1, and tumor glucose metabolism to improve radiotherapy efficacy. *Clin Cancer Res.* 2012;18:5585–5594.

26. Meijer TW, Schuurbiers OC, Kaanders JH, et al. Differences in metabolism between adeno- and squamous cell non-small cell lung carcinomas: spatial distribution and prognostic value of GLUT1 and MCT4. *Lung Cancer.* 2012;76:316–323.

27. Yohena T, Yoshino I, Takenaka T, et al. Upregulation of hypoxia-inducible factor-1alpha mRNA and its clinical significance in non-small cell lung cancer. *J Thorac Oncol.* 2009;4:284–290.

28. Kong FM, Frey KA, Quint LE, et al. A pilot study of [^{18}F]fluorodeoxyglucose positron emission tomography scans during and after radiation-based therapy in patients with non small-cell lung cancer. *J Clin Oncol.* 2007;25:3116–3123.

29. Kubota R, Yamada S, Kubota K, Ishiwata K, Tamahashi N, Ido T. Intratumoral distribution of fluorine-18-fluorodeoxyglucose in vivo: high accumulation in macrophages and granulation tissues studied by microautoradiography. *J Nucl Med.* 1992;33:1972–1980.

30. Huang W, Zhou T, Ma L, et al. Standard uptake value and metabolic tumor volume of ^{18}F-FDG PET/CT predict short-term outcome early in the course of chemoradiotherapy in advanced non-small cell lung cancer. *Eur J Nucl Med Mol Imaging.* 2011;38:1628–1635.

31. Massaccesi M, Calcagni ML, Spitilli MG, et al. 18 F-FDG PET-CT during chemo-radiotherapy in patients with non-small cell lung cancer: the early metabolic response correlates with the delivered radiation dose. *Radiat Oncol.* 2012;7:106.

32. Larson SM, Erdi Y, Akhurst T, et al. Tumor treatment response based on visual and quantitative changes in global tumor glycolysis using PET-FDG imaging: the visual response score and the change in total lesion glycolysis. *Clin Positron Imaging.* 1999;2:159–171.

33. De Ruysscher D, van Baardwijk A, Steevens J, et al. Individualised isotoxic accelerated radiotherapy and chemotherapy are associated with improved long-term survival of patients with stage III NSCLC: a prospective population-based study. *Radiother Oncol.* 2012;102:228–233.